Title	Rapid, low temperature synthesis of germanium nanowires from oligosilylgermane precursors
Authors	Meshgi, Mohammad A.;Biswas, Subhajit;McNulty, David;O'Dwyer, Colm;Verni, Giuseppe A.;O'Connell, John;Davitt, Fionán;Letofsky-Papst, Ilse;Poelt, Peter;Holmes, Justin D.;Marschner, Christoph
Publication date	2017-05-08
Original Citation	Aghazadeh Meshgi, M., Biswas, S., McNulty, D., O'Dwyer, C., Alessio Verni, G., O'Connell, J., Davitt, F., Letofsky-Papst, I., Poelt, P., Holmes, J. D. and Marschner, C. (2017) 'Rapid, Low-Temperature Synthesis of Germanium Nanowires from Oligosilylgermane Precursors', Chemistry of Materials, 29(10), pp. 4351-4360. doi: 10.1021/acs.chemmater.7b00714
Type of publication	Article (peer-reviewed)
Link to publisher's version	10.1021/acs.chemmater.7b00714
Rights	© 2017 American Chemical Society. This document is the Accepted Manuscript version of a Published Work that appeared in final form in Chemistry of Materials, copyright © American Chemical Society after peer review and technical editing by the publisher. To access the final edited and published work see http://pubs.acs.org/doi/abs/10.1021/acs.chemmater.7b00714
Download date	2024-05-14 14:35:43
Item downloaded from	https://hdl.handle.net/10468/4243

Rapid, Low Temperature Synthesis of Germanium Nanowires from Oligosilylgermane Precursors

Mohammad Aghazadeh Meshgi[a], Subhajit Biswas[b,c], David McNulty[b], , Colm O'Dwyer[b], Giuseppe Alessio Verni[b,c], John O'Connell[b,c], Fionán Davitt[b,c], Ilse Letofsky-Papst[d], Peter Poelt[d], Justin D. Holmes[b,c,*] and Christoph Marschner[a,*]

[a]Institute of Inorganic Chemistry, Graz University of Technology, Stremayrgasse 9, Graz, Austria. [b]Department of Chemistry and the Tyndall National Institute, University College Cork, Cork, Ireland. [c]AMBER@CRANN, Trinity College Dublin, Dublin 2, Ireland. [d]Institute of Electron Microscopy and Nanoanalysis, Graz University of Technology, Steyrergasse 17, Graz, Austria.

*To whom correspondence should be addressed: Tel: +43 316873 32112; Fax: +43 316873 1032112; E-mail: christoph.marschner@tugraz.at; j.holmes@ucc.ie

Abstract

New oligosilylgermane compounds with weak Ge-H bonds have been used as precursors for the rapid synthesis of germanium (Ge) nanowires in high yields (>80 %), via a solution-liquid-solid (SLS) mechanism, using indium (In) nanoparticles as a seeding agent over a temperature range between 180 to 380 °C. Even at low growth temperatures, milligram quantities of Ge nanowires could be synthesized over a reaction period of between 5 to 10 minutes. The speed of release of Ge(0) into the reaction environment can be tuned by altering the precursor type, synthesis temperature and the presence or lack of an oxidizing agent, such as tri-*n*-octylphosphine oxide (TOPO). Energy dispersive X-ray analysis showed that silicon

atoms from the precursors were not incorporated into the structure of the Ge nanowires. As both In and Ge facilitate reversible alloying with Li, Li-ion battery anodes fabricated with these nanowires cycled efficiently with specific capacities, i.e. >1000 mAh g^{-1}

Introduction

Ge nanowires have been demonstrated to have numerous applications including nanowire field-effect (FET) transistors[1–3], Schottky solar cells[4] and Li ion batteries[5,6]. Due to the vast application and high research interest in Ge nanowires, different growth strategies have been developed to increase the yield and/or quality of Ge nanowires synthesized.[7] In particular, developing cheap and fast fabrication methods for Ge nanowires in large quantities is important for their incorporate as anode materials in commercially viable Li-ion battery technologies. In this regard, supercritical fluid-liquid-solid (SFLS) approaches have been successfully used to produce Ge nanowires with yields of up to 80 %, but SFLS approaches require high temperatures and pressures and sophisticated equipment which limits the application of such methods.[8] Another less complicated, high temperature approach that generates Ge nanowires in yields up to 53 % is solution-liquid-solid (SLS) growth.[9] Although the reported yield via SLS growth is lower than via SFLS approaches, Ge nanowires production via the SLS approach can occur under atmospheric pressure and do not require high pressure equipment.[9,10] Regardless of the yield, simplicity or complexity of the different solution phase mechanisms the growth of Ge nanowires in general have been reported at high temperatures.[7] High temperature growth is required for many reasons, such as the necessary formation of Ge-Au eutectic alloys (in case of Au seeding nanocrystals), the decomposition of the precursors and the demand for Ge nanowires with high crystal and morphological quality. Although other seeding nanoparticles such as Bi with a low Ge-Bi eutectic temperature have been exploited for the growth of Ge nanowires, low conversion rates of the precursor to Ge nanowires (1.2 %) at 300 °C makes the approach at this temperature inefficient.[11] Hence, even when using low

melting point seeding nanoparticles and perhaps disregarding the quality of the nanowires produced, the thermal stability of the precursor remains an obstacle for the low temperature synthesis of Ge nanowires. In recent years several organometallic precursors have been introduced for growing Ge nanowires in solution phase including alkylgermane,[12] germanium alkoxide[13] and oligosilylgermane[14–16] but none of these precursors were suitable for the low temperature synthesis of Ge nanowires in solution.[7] Meanwhile in the case of oligosilylgermane precursors the presence of silicon atoms in the structure of the precursors previously resulted in the formation of Ge nanowires with a silicon based shell.[14–16]

Additionally, traditional Au seeds are not suitable for the low temperature synthesis (≤ 300 °C) of Ge nanowires due to the high eutectic temperature of the Au-Ge binary system. Thus the use of "type C" low eutectic point growth promoters such as In, Sn, Ga *etc*. are preferable for the depression of the nucleation temperature and hence Ge nanowire growth. In addition, the presence of Au seeds can be detrimental to the electrochemical and electrical properties of Ge nanowires. A previous study on the performance of Au-seeded Si nanowires as anodes for Li-ion batteries demonstrated that the presence of Au seeds resulted in large irreversible capacity loss, poor performance at cycle rates of C/5 and faster, and significant capacity fade.[17] Another study on the electrochemical performance of a composite of SnO_2 and graphene demonstrated that the incorporation of In_2O_3 into SnO_2 can improve the electrochemical properties of SnO_2 and reduce the charge transfer resistance of the electrode leading to enhanced reversible capacity and rate capability.[18] Additionally In was shown to reversibly alloy with Li, accommodating up to 4.33 mol of Li per 1 mol of In.[19,20] Hence the presence of In in Ge nanowires may result in additional storage capacity, making In a far more suitable catalyst than commonly used Au.

This paper introduces new types of oligosilylgermane compounds as precursors for In-catalyzed synthesis of phase-pure Ge nanowires, via a SLS mechanism, without the incorporation of silicon atoms from the precursors into the structure of the nanowires. The

unique characteristics of these new oligosilylgermane precursors make them suitable for the rapid synthesis of Ge nanowires at yields > 80 %, over a temperature between 180 to 380 °C. Energy dispersive X-ray (EDX) analysis showed that In atoms from the seeding nanoparticles were incorporated in the structure of the Ge nanowires at concentrations between 1 to 2 at.%. When compared to Au-seeded Ge nanowires, the nanowires formed from the oligosilylgermane precursors exhibited an enhanced charge capacity when tested electrochemically.

Experimental

The synthesis of the precursor compounds was performed under a nitrogen atmosphere by employing standard Schlenk techniques or using a nitrogen filled glovebox (Innovative Technology, Inc). A column solvent purification system was used to dispense benzene and diethylether within the glovebox. KO^{t}Bu (MERCK, 98 %), 18-crown-6 (Fluka, 99 %), sulfuric acid (Carl Roth, 96 %), ethanol (VWR, 99 %) and tri-*n*-octylphosphine oxide (TOPO) (ABCR, 99 %) were used as received. *n*-dodecane (Sigma-Aldrich, 99 %) and *n*-hexadecane (Amresco, technical grade) were degassed with nitrogen bubbling for 1 hr, whereas oleylamine (OA) (Aldrich, technical grade, 70 %) and squalane (Alfa Aesar, 98 %) were subjected to vacuum conditions before use. Hexakis(trimethylsilyl)digermane[21], tris(trimethylsilyl)[tris(trimethylsilyl)silyl]germane[21] and In nanoparticles[22] were prepared following the published procedures.

Precursor Synthesis

*Synthesis of 1,1,2,2-tetrakis(trimethylsilyl)digermane (precursor **1**):*

A mixture of hexakis(trimethylsilyl)digermane (100 mg, 0.171 mmol), KO^{t}Bu (40 mg, 0.359 mmol) and 18-crown-6 (94 mg, 0.359 mmol) was added to benzene (100 µL) and stirred for 4 hr. Red crystals of oligosilyldigermyldipotassium precipitated slowly from the solution mixture. After decantation, pure crystals were dissolved in benzene and the solution mixture

was added over 10 s to an ice-cooled flask containing diethylether (5 mL) and degassed 2 M sulfuric acid (20 mL). After 5 min the organic layer was transferred with a cannula to another flask containing sodium sulfate to dry the organic phase. The organic phase was then transferred by cannula to another flask. After removal of the volatiles in vacuum, compound **1** (53 mg, 70 %) was obtained as a colorless oil.

^{29}Si, ^{13}C and ^{1}H NMR spectra of precursor **1** are shown in Figures S1 to S3 respectively (see Supporting Information). Anal. Calcd for $C_{12}H_{38}Ge_2Si_4$ 440.04: C, 32.75; H, 8.70. Found: C, 34.39; H, 8.66. MS (70 eV) m/z (%): due to high thermal sensitivity the compound does not survive GC separation.

*Synthesis of bis(trimethylsilyl)[tris(trimethylsilyl)silyl]germane (precursor **2**)*

A mixture of tris(trimethylsilyl)[tris(trimethylsilyl)silyl]germane (100 mg, 0.185 mmol), KO^{t}Bu (22 mg, 0.194 mmol) and 18-crown-6 (52 mg, 0.194 mmol) was dissolved in benzene (100 µL) and stirred for 90 min. After complete conversion, detected by ^{29}Si NMR spectroscopy, the orange solution of oligosilylgermylpotassium was added over 10 s to an ice-cooled flask containing diethylether (5 mL) and degassed 2 M sulfuric acid (20 mL). After 5 min the organic phase was transferred by cannula to another flask containing sodium sulfate to dry the organic phase. The organic phase was transferred by cannula to another flask. After removal of the volatiles in vacuum compound **2** (67 mg, 7 %) was obtained as a colorless oil.

^{29}Si, ^{13}C and ^{1}H NMR spectra of the precursor **2** are shown in Figure S4 to S6 respectively (see Supporting Information). Anal. Calcd for $C_{15}H_{46}GeSi_6$ 467.67: C, 38.52; H, 9.91. Found: C, 39.17; H, 9.78. MS (70eV) m/z (%): 394(31)[$C_{12}H_{36}GeSi_5^+$]; 305(6)[$C_8H_{23}GeSi_4^+$]; 245(15)[$C_9H_{25}Si_4^+$]; 206(10)[$C_5H_{16}GeSi_2^+$]; 171(14)[$C_6H_{15}Si_3^+$]; 147(3)[$GeSiMe_3^+$]; 73(100)[$SiMe_3^+$].

Synthesis of Ge Nanowires

Depending on the experiment, trioctylphosphine oxide (TOPO) or oleylamine (OA) was transferred to a Schlenk tube and then the appropriate high boiling solvent, *e.g. n*-dodecane, *n*-hexadecane or squalane was added to the tube. To heat the tube a LOSA model tube furnace from HTM Reetz GmbH was used. After adjusting the temperature, a colloidal solution of In nanoparticles with a mean diameter of 6.4 ± 0.4 nm, was injected into the Schlenk tube followed by precursor injection 30 s later (at low synthesis temperatures or immediate injection of precursors at high synthesis temperatures). Precursor **1** or **2** was taken as follows: precursor **1** (79 mg, 0.18 mmol) or precursor **2**: (25 mg, 0.05 mmol) was dissolved in toluene (100 µL) and then was injected into the Schlenk tube. Due to the differing thermal sensitivities and reactivities of precursors **1** and **2**, for precursor **1** the tube was left inside the furnace for 5 min and for the more stable precursor **2**, it was left in the furnace for 10 min. At the end of the reaction the tube was brought out of the furnace and left in air to cool down to room temperature. After centrifugation of the reaction mixture in the presence of ethanol the solid obtained was subjected to further analysis.

Electrochemical Experiments

All electrochemical data presented in this report were performed using a BioLogic VSP Potentiostat/Galvanostat. The electrochemical properties of Ge nanowires grown with precursor **1** at 180 °C were investigated in a half-cell configuration against a pure Li counter electrode in a two electrode, stainless steel split cell (a coin cell assembly that can be disassembled for post-mortem analysis). The electrolyte used consisted of a 1 mol dm^{-3} solution of lithium hexafluorophosphate salt in a 1:1 (v/v) mixture of ethylene carbonate in dimethyl carbonate with 3 wt.% vinylene carbonate. The separator used in all split cell tests was a glass fibre separator (El-Cell ECC1-01-0012-A/L, 18 mm diameter, 0.65 mm thickness). Working electrodes consisted of Ge nanowire powder dropcast onto Cu foil. The mass loading for all

Ge nanowire samples was ~ 1.0 mg. Cyclic voltammetry was performed using a scan rate of 0.2 mV s^{-1} in a potential window of 1.5 – 0.01 V. Galvanostatic cycling was performed using a C rates of C/20 in a potential window of 1.5 – 0.01 V.

Analytical Methods

Nuclear magnetic resonance (NMR) spectroscopy was performed on a Varian INOVA 300 (^{1}H 299.95 MHz, ^{13}C 75.43 MHz and ^{29}Si 59.59 MHz) spectrometer. Samples were dissolved in benzene-d_6 or in the case of a non-deuterated solvent a capillary filled with D_2O was used for deuterium lock. Shifts are reported in ppm downfield from tetramethylsilane and are referenced to solvent residual signals. To compensate for the low isotopic abundance of ^{29}Si, the INEPT pulse sequence[23,24] was used for the amplification of the signal.

Scanning electron microscopy (SEM) was performed using a Zeiss DSM 982 Gemini or FEI Helios NanoLab 600i both equipped with field emission gun. The images were mainly recorded with the Everhart-Thornley detector (secondary electron images), some were recorded with the solid state detector (backscattered electrons images). , providing materials contrast.

Energy dispersive X-ray (EDX) measurements were undertaken in high angle annular dark-field (HAADF) mode on a FEI Helios NanoLab 600i operating at 10 kV and 0.69 nA, equipped with an Oxford X-Max 80 detector. EDX measurements to calculate the In concentration in the nanowires were performed in "point" mode on single nanowires. Error in the EDX measurements of the Ge nanowires indicates the standard deviation measured over 20 nanowires. The detection sensitivity of EDX analysis is around 0.1 wt%.

Transmission electron microscopy (TEM) was conducted on a T12 microscope from FEI operated at 120 kV with LaB_6 cathode, a monochromated TF20 microscope from FEI operated at 200 kV with a Schottky cathode or JEOL 2100 operated at 200 kV with LaB_6 electron source. The TF20 microscope for X-ray spectroscopy was equipped with a SiLi

detector with ultrathin window and for electron energy loss spectroscopy with a high-resolution Gatan imaging filter (GIF).

X-ray diffraction (XRD) was performed on a Philips X'pert Pro MPD with a Panalytical Empyrean Cu X-ray tube with a Philips X'celerator detector. Spectra were acquired with an energy setting of 40 kV and 35 mA, fixed divergence slit of 1° and with a Ni filter on the diffracted optics. Ge powder (99.999 %) with 200 mesh from Haines & Maassen Metallhandelsgesellschaft GmbH was used as bulk Ge to be compared with Ge nanowires.

Gas chromatography was carried out on an Agilent 7890A (capillary column HP-5MS; 30 m × 0.250 mm; Film 0.25µm) with mass spectrometer Agilent 5975C. Assignment of mass spectra was either accomplished by comparison to data from a database or alternatively for mass spectra not covered by the library, compound analysis was carried out using standard techniques for interpretation of mass spectra.[25]

Elemental analysis was carried out using a Heraeus VARIO ELEMENTAR instrument.

Raman spectroscopy was performed on Raman Station 400F from Perkin Elmer equipped with 350 mW near infrared 785 nm laser. Ge nanowires of each sample were transferred to a glass capillary and were measured with 28 mW of the laser power.

Results and Discussion

Synthesis of Ge nanowires using 1,1,2,2-tetrakis(trimethylsilyl)digermane (precursor 1)

Thermal decomposition of diluted precursor **1** in *n*-dodecane was observed after 30 min at 170 °C as the initially transparent solution turned to yellow/brown and later a yellow/brown precipitate appeared at the bottom of the reaction flask. The solution obtained was analyzed using ^{29}Si NMR spectroscopy and only the baseline was observed, indicating the decomposition of the precursor. Moreover, GC-mass spectrometry of pure precursor **1** showed only tris(trimethylsilyl)silane and tetrakis(trimethylsilyl)germane without any sign of precursor **1** indicating its high thermal sensitivity and decomposition. Thermal decomposition of precursor

1 at low temperatures, in contrast to the thermally stable diphenylgermane (DPG),[9,26] makes it an appropriate candidate for low temperature synthesis of Ge nanowires.

For seed-mediated synthesis of Ge nanowires at low temperatures, a suitable precursor which can release reactive Ge atoms at low temperatures is extremely important. Additionally, metallic seeds also have a significant role. For the successful low temperature synthesis of Ge nanowires the metallic seed should have a low temperature eutectic point in the metal-Ge binary phase diagram. The binary phase diagram of Ge-In displays a significant decrease in the eutectic point at 156 °C[27] compared to Au-Ge eutectic temperature at 363 °C. This very low eutectic temperature of In-Ge binary system predicts that In nanoparticles are ideal seeds for low temperature growth of Ge nanowires.

Although precursor **1** was found to decompose at low temperatures, the synthesis of Ge nanowires was performed at various temperatures such as 180, 300, 350 and 380 °C to investigate the effect of temperature on the morphology of the nanowires. With respect to the synthesis temperature and the boiling point of the solvents the reaction was performed in different solvents such as *n*-dodecane, *n*-hexadecane or squalane in the presence of capping ligands such as TOPO or OA. Figures 1(a) and (b) show SEM and high resolution bright field TEM images of a sample prepared in the presence of a TOPO capping ligand at 180 °C. Curly and worm-like nanowires were observed, similar in morphology to the worm-like nanowires previously reported by Ryan and co-workers at temperatures above 400 °C.[26] TEM analysis confirmed the nanowires were crystalline in nature with random crystal defects (Figure 1(b)). The dark round sphere at the tip of the nanowire (Figure 1(b) inset) corresponds to the In nanoparticle seed and confirms seed-mediated growth of the Ge nanowire. The mass of Ge nanowires obtained in this reaction was 21.0 mg. Considering the weight of the In nanoparticles (~ 0.41 mg), the yield of the Ge nanowires was 81 % (Table 1). This yield of Ge nanowires synthesized at low temperature is higher than those previously reported via SLS growth using GeI_2 or DPG as precursors, with 40 %[9] or 52.8 %[10] yield respectively.

To study the effect of temperature on the morphology of the Ge nanowires the synthesis temperature was raised to 300 and 380 °C, while keeping other parameters the same. At 300 °C irregular and highly agglomerated Ge nanowires and at 380 °C fine Ge nanoparticles instead of nanowires were obtained (Figure S7, see Supporting Information). According to the SEM analysis, nanowires with a good morphology were obtained at 180 °C and increasing the synthesis temperature to 380 °C changed the structure from nanowires to nanoparticles. The weight of the product at 300 and 380 °C was approximately 21 mg for both cases.

Furthermore, the type of capping ligand and its effect on the morphology of Ge nanowires were studied by replacing TOPO with OA while keeping other parameters constant, apart from temperature. The highest synthesis temperature was decreased from 380 to 350 °C in the case of OA due to the lower boiling point of OA (≈350 °C), when compared to TOPO. Figure 2 shows the SEM images of Ge nanowires synthesized at different temperatures in the presence of OA. Figure 2(a) relates to a sample prepared at 180 °C. According to the SEM image the sample contained highly agglomerated Ge nanowires with a yield of 23 %. The low yield obtained in this experiment in comparison to the experiment with TOPO at 180 °C with the yield of 81 %, shows the low conversion of the precursor to Ge nanowires in the absence of TOPO.

Figure 2(b) displays Ge nanowires prepared in the presence of OA at 300 °C. According to SEM analysis these sample contained curly Ge nanowires with undulating surfaces. Although this reaction was performed in the absence of TOPO, the reaction yield obtained was 77 % (Table 1). Hence, the conversion of the precursor to Ge nanowires at 300 °C can take place even in the absence of TOPO. Ge nanowires were also synthesized in the presence of OA at 350 °C (Figure 2(c)). Figure 2(c) depicts curly Ge nanowires with undulating surfaces forming at this temperature. Increasing the synthesis temperature from 300 to 350 °C increased the reaction yield from 77 to 85 % (Table 1).

Figure 3 shows bright field TEM images and selected area electron diffraction (SAED) patterns of the Ge nanowires synthesized in the presence of OA at 300 and 350 °C. A considerable amount of random stacking faults, parallel to the nanowire growth axis, was observed (Figures 3(a), (b) and (d)) in the Ge nanowires synthesized at both temperatures with OA. In addition, SAED patterns recorded from the nanowires, inset of Figure 3(a) and 3(d), showed additional reflections, which relate to the presence of stacking faults in the structure of Ge nanowires. Bright field high-resolution transmission electron microscopy (HRTEM) analysis (Figure 3(c)) also confirmed the high crystallinity of a Ge nanowire with 1.8 at.% In incorporation synthesized with OA. Fast Fourier transform (FFT) analysis showed (in the inset of Figure 3(c)) a pseudo hexagonal symmetry with reflections assigned to the high-order Laue zone diffraction of {111} in diamond cubic crystals. FFT and HRTEM images depicted an interplanar spacing (*d*) between {111} planes in the nanowires to be around 0.328 nm, which is larger than the *d* value for bulk diamond Ge crystal (JCPDS 04-0545). An increase in the *d* value from bulk Ge is expected with the incorporation of large amounts of In in the Ge lattice. In general, according to the reaction yields and morphology of the Ge nanowires, TOPO was found to be a suitable capping ligand for synthesizing nanowires at low temperatures, such as 180 °C, but in contrast OA was found to be a suitable capping ligand for synthesizing nanowires at higher temperatures, such as 300 and 350 °C.

Table 1 summarizes the amount of In incorporation in different Ge nanowire samples according to EDX analysis. In the case of the nanowires synthesized with precursor **1** the In content in the structure of the nanowires increased from 1.3 ± 0.1 to 1.8 ± 0.8 at% by raising the synthesis temperature from 180 to 350 °C respectively, as shown in Figure S8(a) (see Supporting Information). In addition, EDX analysis showed that the Ge nanowires synthesized at different growth conditions only consisted of Ge and a small quantity of In atoms, without the presence of silicon atoms (Figure S8(b), see Supporting Information) or at least below detection sensitivity. EDS mapping also confirmed that the SLS-grown nanowires only

consisted of Ge and In atoms (Figure S9, see Supporting Information). As the silicon atoms of the precursor did not incorporate into structure of Ge nanowires the solution phase was studied to determine the fate of the silicon atoms, which will be discussed in detail later.

Synthesis of Ge nanowires using bis(trimethylsilyl)[tris(trimethylsilyl)silyl]germane (precursor 2)

In contrast to precursor **1** which was not detected using GC-MS analysis due to its high thermal sensitivity, precursor **2** was characterized using GC-MS analysis. Diluted solutions of the precursor **2** in *n*-dodecane remained colorless after heating for 30 min at 170 °C. ^{29}Si NMR spectroscopy of these solutions suggested that precursor **2** was intact in the solution. These results clearly indicated a much improved thermal stability of the precursor **2** in comparison to the precursor **1**.

Initially the synthesis of Ge nanowires with precursor **2** was performed at 180 °C in the presence of either TOPO or OA and in both cases colorless solutions without the formation of any brown/black solid, related to Ge nanowires, were observed. The same phenomenon was also observed at 300 °C. As no Ge nanowires were formed, due to the higher thermal stability of the precursor **2** in comparison to the precursor **1**, further synthesis of Ge nanowires with precursor **2** was performed at 350 °C. The synthesis of Ge nanowires at this temperature was only performed in the presence of OA as it was previously observed that TOPO has a negative effect on the morphology of the Ge nanowires at elevated temperatures.

Figure 4 displays SEM and bright field TEM images of Ge nanowires synthesized with precursor **2** at 350 °C. Instead of the curly nanowires previously obtained with precursor **1** (Figures 1, 2 and 3), Ge nanowires synthesized with precursor **2** were straighter with smooth surfaces (Figure 4). However, a few curly and kinked nanowires were also observed (Figure 4(c)). The dark round sphere at the tip of the nanowire (Figure 4(d)) confirmed seed-mediated growth of the Ge nanowires. The inset shows the FFT pattern of a single crystalline Ge

nanowire grown from an In nanoparticle with precursor **2.** The weight of the product obtained with precursor **2** at 350 °C was 3.1 mg. The weight of the In nanoparticles was measured as (~ 0.06 mg) and the yield of the Ge nanowires was 79 %, which is very close to the yield of the Ge nanowires obtained with precursor **1** (Table 1).

Figure 5 shows histograms of Ge nanowires diameters synthesized at different growth conditions. Figures 5 (a)-(c) relate to the three samples prepared with precursor **1** at different synthesis temperatures with diameter ranging between 20 to 140 nm. Comparison between the three histograms shows that an increase of the synthesis temperature from 180 °C to 350 °C slightly increases the mean diameter of the nanowires from 71 to 78 nm, respectively. Figure 5(d) shows the histogram of a sample synthesised with precursor **2** at 350 °C, with diameters ranging between 30 to 110 nm. The mean diameter of the nanowires of in this sample was 56 nm which is smaller than the mean diameter of samples made at the same temperature using precursor **1**. This highlights that beside the synthesis temperature, the type of the precursor can affect the mean diameter of nanowires.

EDX analysis of Ge nanowires grown with precursor **2** showed approximately 0.9 ± 0.1 at% In within the Ge nanowires (Table 1). To further confirm the presence of In in the structure of the nanowires XRD and Raman spectroscopy were performed on Ge nanowire samples. A higher incorporation of In in the structure of Ge nanowires can increase the red shift in the Raman spectra of the nanowires (Figure S10, see Supporting Information). In addition, the mismatch between the XRD pattern of bulk Ge with Ge nanowires incorporating In (Figure S11, see Supporting Information) was in accordance with Vegard's law and confirmed the effect of In incorporation in the Ge matrix (see Supporting Information).

Fate of the silicon atoms and the decomposition mechanism of oligosilylgermane precursors

According to EDX analysis, similar to the Ge nanowires prepared with precursor **1**, silicon atoms were not detected in Ge nanowires prepared with precursor **2**. As the silicon atoms of the precursor did not incorporate into the structure of the Ge nanowires, the solution phase of the reactions involving precursor **1** with TOPO and OA were separately analysed by NMR spectroscopy to investigate the fate of the silicon atoms from the precursor. According to ^{29}Si NMR spectroscopy of the solution phase containing TOPO, the peak from precursor **1** at -5.7 ppm vanished (Figure S1, see Supporting Information) and a peak at 6.9 ppm appeared (Figure S12, see Supporting Information), which can be assigned to hexamethyldisiloxane.[28] This change suggestrs that the free trimethylsilyl (TMS) groups of the precursor reacted with oxygen atoms and were trapped in the solution phase. As the reaction was performed under nitrogen atmosphere with degassed solvents, TOPO can be regarded as the main source of oxygen. In the case of the solution phase containing OA, the ^{29}Si NMR spectrum showed a large peak at 1.6 ppm and a very small peak at 6.9 ppm (Figure S13, see Supporting Information) confirming again the presence of TMS groups in the solution phase. Independent synthesis of trimethylsilyloleylamine showed that it corresponds to the NMR signal at 1.6 ppm (Figure S13, see Supporting Information). The small signal at 6.9 ppm can be assigned to hexamethyldisiloxane forming through the presence of trace amounts of oxygen, most likely coming from impurities within the technical grade OA. Figure 6 displays a mechanism for the thermal decomposition of the oligosilylgermane precursors, subsequent reaction of the TMS groups with the existing capping ligands inside the solution and finally the formation of the In-catalyzed Ge nanowires.

As outlined above (Figure S14, see Supporting Information) the reaction of the TMS groups of the precursor with oxygen from TOPO was confirmed by ^{29}Si NMR. In the presence of TOPO when the synthesis temperature was raised from 180 to 300 °C and finally to 380 °C, instead of discrete nanowires, agglomerated solid or nanoparticles formed. Moreover, in a

separate experiment, the addition of a small quantity of TOPO to the reaction involving the synthesis of Ge nanowires in the presence of OA at 350 °C, changed the morphology of the final product from nanowires to particles (Figure S15, see Supporting Information). Observations of different morphological features at different temperatures lead to the conclusion that besides the thermal decomposition of precursor **1**, oxidation of precursor **1** with TOPO has a profound effect on the decomposition rate and the formation of the reactive Ge(0) species. As the synthesis temperature increases, facile reaction of the TMS groups from precursor **1** with TOPO causes a burst of reactive Ge(0) species into the reaction. This burst causes an instantaneous increase in the concentration of Ge(0) species in the reaction environment that cannot be completely absorbed by the In nanoparticles to form nanowires, therefore excess Ge(0) species spontaneously accumulate to form irregular solids or particles. The very poor yield (23 %) of Ge nanowires synthesized in the presence of OA at 180 °C indicates that the appropriate decomposition of precursor **1** and the formation of Ge(0) at low temperatures requires a driving force, *i.e.* the reaction of TMS groups with the oxygen of TOPO.

High level of In incorporation in Ge nanowires

In contrast to the binary phase diagram of Ge-In, with negligible solid solubility of In in Ge,[27] in the current study incorporation of approximately 2 at% In in the structure of Ge nanowires was observed. Non-equilibrium incorporation of a high level of In atoms in Ge nanowires can be explained via the solute trapping mechanism aided by rapid and diffusionless solidification processes. Rapid solidification during VLS crystal growth causes the impurity or the solute to be trapped in the matrix at higher amounts than the equilibrium solidification can predict.[29] At the catalyst-nanowire interface, In impurity adatoms are trapped on the high energy sites of the crystal lattice, leading to the formation of a metastable solid (Ge-In alloy) at the nanowire growth front. The formation and growth of Ge nanowires is driven with the step initiation at the nanowire-catalyst interface and step-flow kinetics.[30,31] The rapid formation of steps and

also the high step velocity enhances the impurity, or the solute trapping, and its incorporation into the matrix.[32,33] Rapid formation of Ge nanowires with oligosilylgermane precursors provides a high step velocity during the synthesis of the nanowires which enhances the probability of In adatoms being trapped at the catalyst-nanowire interface with the fast deposition of successive layers during nanowire growth. The fact that nanowires with faster growth kinetics, synthesized with precursor **1** over 5 min reaction time, exhibited higher In incorporation (1.8 at%) compared to nanowires with slower growth rates synthesized with precursor **2** over a 10 min reaction time (0.9 at%), is evidence that kinetic-dependent solute trapping of In incorporation in the Ge nanowire lattice is happening.

Electrochemical experiments of Ge nanowires synthesised with precursor 1 at 180 °C

In order to investigate the electrochemical performance of the In-catalysed Ge nanowires as Li-ion battery anodes, cyclic voltammetry and galvanostatic tests were performed as shown in Figure 7. The first three CV scans are shown in Figure 7(a). Two weak peaks were observed in the first anodic scan at ~ 1.11 and 0.68 V, which may be associated with the formation of a solid electrolyte interface (SEI) layer.[34] A sharp reduction peak was observed at ~ 0.14 V, corresponding to the formation of a Li-Ge alloy during the anodic scan.[35] Weak shoulder peaks were also observed at ~ 0.21, 0.18 and 0.07 V, indicating that a number of different and successively higher Li-mole fraction Li-Ge alloyed phases were formed during electrochemical lithiation.[36] From the second cycle onwards the reduction peak was shifted to a slightly lower potential of ~ 0.11 V and also became broader. A broadening of the anodic peaks after the first cycle has previously been attributed to a conversion of crystalline Ge to amorphous Ge in tandem with delithitation processes.[37] A strong oxidation peak was observed in the first cathodic scan at ~ 0.59 V corresponding to the phase transition from Li_xGe to Ge.[38]

Galvanostatic tests were performed in order to further evaluate the electrochemical performance of the In-catalyzed Ge nanowires, in terms of specific capacity values and capacity

retention during charge-discharge cycling. The galvanostatic charge and discharge curves for the 1st, 2nd, 10th and 15th cycles for Ge nanowires at a C/20 rate are shown in Figures 7(b) and (c). A sloping region in the first charge curve was observed from ~ 2.73 – 0.35 V, which may be attributed to the formation of an SEI layer and the irreversible decomposition of the electrolyte on the surface of the electrode material.[1] This is followed by a distinct long plateau at ~ 0.3 V, corresponding to the alloying of the Ge nanowires with Li.[39] A long plateau was also observed in the first discharge curve at ~ 0.52 V corresponding to the dealloying of the Ge nanowires, which is in close agreement with the potential at which the strong oxidation peak occurred in the first anodic CV scan, shown in Figure 7(a).

The specific capacity values obtained over fifteen cycles are shown in Figure 7(d). The initial charge and discharge capacities obtained were ~ 2678.9 and 1169.9 mAh/g respectively, corresponding to a coulombic efficiency (CE) of ~ 43.7 %. The low initial CE can be attributed to considerable volume changes of the Ge nanowires during alloying with Li, which may result in the loss of electrical contact with the current collector.[40] The capacities for the second charge and discharge decreased to ~ 1236.2 and 1219.5 mAh/g respectively. Similar differences between the capacities obtained for the first and second charge have previously been reported for various Ge nanostructures.[39,41] However, from the second cycle onwards the capacity retention was greatly improved achieving charge capacities of ~ 1008.1 and 920.5 mAh/g after the 10th and 15th charges, respectively. The significant difference in the specific capacity for the initial charge and subsequent cycles may be attributed to the formation of an SEI layer and local structure rearrangement in the nanowires to accommodate the mechanical stress induced during alloying and dealloying.[37] The capacities values obtained over 15 cycles were greater than previously reported values for Au-seeded Ge nanowires[36,42] and comparable to values reported for Ge nanowires catalyszd with Sn , and like In, it also reversibly alloys with Li.[6] Previous reports indicate that Au does not reversibly alloy with lithium causing Au-seeded Ge nanowires to suffer from significant capacity fading issues.[17] In has previously been shown to

reversibly alloy with Li, accommodating up to 4.33 mol of Li per 1 mol of In,[19] hence it is clear that the increased capacities obtained for our Ge nanowires, compared to Au-seeded nanowires, are due to the presence of In. This indicates that In is a suitable alternative catalyst to commonly used Au and also that In-seeded Ge nanowires formed quickly at relatively low temperatures, are a promising anode material for Li ion batteries.

Conclusion

High yield synthesis of In-catalysed Ge nanowires with new oligosilylgermane precursors as Ge sources was performed using the SLS mechanism in a temperature range between 180 and 380 °C. At high synthesis temperatures, a notable yield of 85 % was obtained. However, to obtain the same yield at low temperatures, the presence of an oxidising agent such as TOPO was necessary. As trimethylsilyl groups of the precursor react with OA or oxygen from TOPO, the silyl groups remain in the solution phase and do not interfere with nanowire formation. EDX analysis showed no silicon impurity existed in the structure of the Ge nanowires and only the presence of approximately 1 to 2 at.% of In. Rapid synthesis of Ge nanowires with new oligosilylgermane precursors enhances the solute trapping phenomenon and increases the incorporation of In atoms in Ge nanowires. Electrochemical testing also showed that the incorporation of In atoms in Ge nanowires greatly enhances the charge capacity of the nanowires in comparison to previously reported values for Ge nanowires synthesized with Au seeds.

Associated content

Supporting information

Detailed discussion on indium incorporation in Ge nanowires, NMR spectra of precursors, SEM images of Ge nanowires synthesized in the presence of TOPO at high synthesis temperatures, EDX spectrum and mapping of a single Ge nanowire, Raman spectra and XRD spectrum, ^{29}Si NMR spectra of the reactions and finally SEM image of Ge nanowires synthesized in presence of OA and TOPO mixture at high synthesis temperature.

Acknowledgments

Support for this study was provided by the Austrian *Fonds zur Förderung der wissenschaftlichen Forschung* (FWF) via the projects P-22678 and P-26417 and Science Foundation Ireland (grant: 14/IA/2513).

References

(1) Wang, D.; Wang, Q.; Javey, A.; Tu, R.; Dai, H.; Kim, H.; McIntyre, P. C.; Krishnamohan, T.; Saraswat, K. C. Germanium Nanowire Field-Effect Transistors with SiO2 and High-κ HfO2 Gate Dielectrics. *Appl. Phys. Lett.* **2003**, *83*, 2432–2434.

(2) Tang, J.; Wang, C.-Y.; Xiu, F.; Zhou, Y.; Chen, L.-J.; Wang, K. L. Formation and Device Application of Ge Nanowire Heterostructures via Rapid Thermal Annealing. *Adv. Mater. Sci. Eng.* **2011**, *2011*, Article ID 316513.

(3) Tang, J.; Wang, C.-Y.; Hung, M.-H.; Jiang, X.; Chang, L.-T.; He, L.; Liu, P.-H.; Yang, H.-J.; Tuan, H.-Y.; Chen, L.-J.; Wang, K. L. Ferromagnetic Germanide in Ge Nanowire Transistors for Spintronics Application. *ACS Nano* **2012**, *6*, 5710–5717.

(4) Yun, J.-H.; Park, Y. C.; Kim, J.; Lee, H.-J.; Anderson, W. A.; Park, J. Solution-Processed Germanium Nanowire-Positioned Schottky Solar Cells. *Nanoscale Res. Lett.* **2011**, *6*, 287.

(5) Armstrong, M. J.; O'Dwyer, C.; Macklin, W. J.; Holmes, J. D. Evaluating the Performance of Nanostructured Materials as Lithium-Ion Battery Electrodes. *Nano Res.* **2013**, *7*, 1–62.

(6) Kennedy, T.; Mullane, E.; Geaney, H.; Osiak, M.; O'Dwyer, C.; Ryan, K. M. High-Performance Germanium Nanowire-Based Lithium-Ion Battery Anodes Extending over 1000 Cycles Through in Situ Formation of a Continuous Porous Network. *Nano Lett.* **2014**, *14*, 716–723.

(7) Geaney, H.; Mullane, E.; Ryan, K. M. Solution Phase Synthesis of Silicon and Germanium Nanowires. *J. Mater. Chem. C* **2013**, *1*, 4996–5007.

(8) Hanrath, T.; Korgel, B. A. Nucleation and Growth of Germanium Nanowires Seeded by Organic Monolayer-Coated Gold Nanocrystals. *J. Am. Chem. Soc.* **2002**, *124*, 1424–1429.

(9) Chockla, A. M.; Korgel, B. A. Seeded Germanium Nanowire Synthesis in Solution. *J. Mater. Chem.* **2009**, *19*, 996–1001.

(10) Lu, X.; Fanfair, D. D.; Johnston, K. P.; Korgel, B. A. High Yield Solution−Liquid−Solid Synthesis of Germanium Nanowires. *J. Am. Chem. Soc.* **2005**, *127*, 15718–15719.

(11) Chockla, A. M.; Harris, J. T.; Korgel, B. A. Colloidal Synthesis of Germanium Nanorods. *Chem. Mater.* **2011**, *23*, 1964–1970.

(12) Zaitseva, N.; Dai, Z. R.; Grant, C. D.; Harper, J.; Saw, C. Germanium Nanocrystals Synthesized in High-Boiling-Point Organic Solvents. *Chem. Mater.* **2007**, *19*, 5174–5178.

(13) Gerung, H.; Boyle, T. J.; Tribby, L. J.; Bunge, S. D.; Brinker, C. J.; Han, S. M. Solution Synthesis of Germanium Nanowires Using a Ge2+ Alkoxide Precursor. *J. Am. Chem. Soc.* **2006**, *128*, 5244–5250.

(14) Hobbs, R. G.; Barth, S.; Petkov, N.; Zirngast, M.; Marschner, C.; Morris, M. A.; Holmes, J. D. Seedless Growth of Sub-10 Nm Germanium Nanowires. *J. Am. Chem. Soc.* **2010**, *132*, 13742–13749.

(15) Lotty, O.; Hobbs, R.; O'Regan, C.; Hlina, J.; Marschner, C.; O'Dwyer, C.; Petkov, N.; Holmes, J. D. Self-Seeded Growth of Germanium Nanowires: Coalescence and Ostwald Ripening. *Chem. Mater.* **2013**, *25*, 215–222.

(16) Arnold, D. C.; Hobbs, R. G.; Zirngast, M.; Marschner, C.; Hill, J. J.; Ziegler, K. J.; Morris, M. A.; Holmes, J. D. Single Step Synthesis of Ge–SiOx Core-Shell Heterostructured Nanowires. *J. Mater. Chem.* **2009**, *19*, 954–961.

(17) Chockla, A. M.; Bogart, T. D.; Hessel, C. M.; Klavetter, K. C.; Mullins, C. B.; Korgel, B. A. Influences of Gold, Binder and Electrolyte on Silicon Nanowire Performance in Li-Ion Batteries. *J. Phys. Chem. C* **2012**, *116*, 18079–18086.

(18) Yang, H.; Song, T.; Lee, S.; Han, H.; Xia, F.; Devadoss, A.; Sigmund, W.; Paik, U. Tin Indium Oxide/graphene Nanosheet Nanocomposite as an Anode Material for Lithium

Ion Batteries with Enhanced Lithium Storage Capacity and Rate Capability. *Electrochimica Acta* **2013**, *91*, 275–281.

(19) Ho, W.-H.; Li, C.-F.; Liu, H.-C.; Yen, S.-K. Electrochemical Performance of In2O3 Thin Film Electrode in Lithium Cell. *J. Power Sources* **2008**, *175*, 897–902.

(20) Osiak, M.; Khunsin, W.; Armstrong, E.; Kennedy, T.; Torres, C. M. S.; Ryan, K. M.; O'Dwyer, C. Epitaxial Growth of Visible to Infra-Red Transparent Conducting In 2 O 3 Nanodot Dispersions and Reversible Charge Storage as a Li-Ion Battery Anode. *Nanotechnology* **2013**, *24*, 65401.

(21) Fischer, J.; Baumgartner, J.; Marschner, C. Silylgermylpotassium Compounds. *Organometallics* **2005**, *24*, 1263–1268.

(22) Aghazadeh Meshgi, M.; Kriechbaum, M.; Biswas, S.; Holmes, J. D.; Marschner, C. Synthesis of Indium Nanoparticles at Ambient Temperature; Simultaneous Phase Transfer and Ripening. *J. Nanopart. Res.* **2016**, *18*, 363.

(23) Morris, G. A.; Freeman, R. Enhancement of Nuclear Magnetic Resonance Signals by Polarization Transfer. *J. Am. Chem. Soc.* **1979**, *101*, 760–762.

(24) Helmer, B. J.; West, R. Enhancement of Silicon-29 NMR Signals by Proton Polarization Transfer. *Organometallics* **1982**, *1*, 877–879.

(25) McLafferty, F. W. *Interpretation of Mass Spectra*; University science books, Mill valley, Ca, 1980.

(26) Geaney, H.; Dickinson, C.; Weng, W.; Kiely, C. J.; Barrett, C. A.; Gunning, R. D.; Ryan, K. M. Role of Defects and Growth Directions in the Formation of Periodically Twinned and Kinked Unseeded Germanium Nanowires. *Cryst. Growth Des.* **2011**, *11*, 3266–3272.

(27) Olesinki, R. W.; Kanani, N.; Abbaschian, G. J. The Ge-In (Germanium-Indium) System. *Bull. Alloy Phase Diagr.* **1985**, *6*, 536–539.

(28) Rohde, M.; Müller, L. O.; Himmel, D.; Scherer, H.; Krossing, I. A Janus-Headed Lewis Superacid: Simple Access To, and First Application of Me3Si-F-Al(ORF)3. *Chem. Eur. J.* **2014**, *20*, 1218–1222.

(29) Galenko, P. Solute Trapping and Diffusionless Solidification in a Binary System. *Phys. Rev. E* **2007**, *76*, 31606.

(30) Wen, C.-Y.; Tersoff, J.; Reuter, M. C.; Stach, E. A.; Ross, F. M. Step-Flow Kinetics in Nanowire Growth. *Phys. Rev. Lett.* **2010**, *105*, 195502.

(31) Golovin, A. A.; Davis, S. H.; Voorhees, P. W. Step-Flow Growth of a Nanowire in the Vapor-Liquid-Solid and Vapor-Solid-Solid Processes. *J. Appl. Phys.* **2008**, *104*, 74301.

(32) Moutanabbir, O.; Isheim, D.; Blumtritt, H.; Senz, S.; Pippel, E.; Seidman, D. N. Colossal Injection of Catalyst Atoms into Silicon Nanowires. *Nature* **2013**, *496*, 78–82.

(33) Biswas, S.; Doherty, J.; Saladukha, D.; Ramasse, Q.; Majumdar, D.; Upmanyu, M.; Singha, A.; Ochalski, T.; Morris, M. A.; Holmes, J. D. Non-Equilibrium Induction of Tin in Germanium: Towards Direct Bandgap Ge1−xSnx Nanowires. *Nat. Commun.* **2016**, *7*, 11405.

(34) Fang, S.; Shen, L.; Zheng, H.; Zhang, X. Ge–graphene–carbon Nanotube Composite Anode for High Performance Lithium-Ion Batteries. *J. Mater. Chem. A* **2014**, *3*, 1498–1503.

(35) Wang, J.; Du, N.; Zhang, H.; Yu, J.; Yang, D. Cu–Ge Core–shell Nanowire Arrays as Three-Dimensional Electrodes for High-Rate Capability Lithium-Ion Batteries. *J. Mater. Chem.* **2011**, *22*, 1511–1515.

(36) Tan, L. P.; Lu, Z.; Tan, H. T.; Zhu, J.; Rui, X.; Yan, Q.; Hng, H. H. Germanium Nanowires-Based Carbon Composite as Anodes for Lithium-Ion Batteries. *J. Power Sources* **2012**, *206*, 253–258.

(37) Li, W.; Yang, Z.; Cheng, J.; Zhong, X.; Gu, L.; Yu, Y. Germanium Nanoparticles Encapsulated in Flexible Carbon Nanofibers as Self-Supported Electrodes for High Performance Lithium-Ion Batteries. *Nanoscale* **2014**, *6*, 4532–4537.

(38) Liu, X.; Hao, J.; Liu, X.; Chi, C.; Li, N.; Endres, F.; Zhang, Y.; Li, Y.; Zhao, J. Preparation of Ge Nanotube Arrays from an Ionic Liquid for Lithium Ion Battery Anodes with Improved Cycling Stability. *Chem. Commun.* **2015**, *51*, 2064–2067.

(39) Chan, C. K.; Zhang, X. F.; Cui, Y. High Capacity Li Ion Battery Anodes Using Ge Nanowires. *Nano Lett.* **2008**, *8*, 307–309.

(40) Yuan, F.-W.; Yang, H.-J.; Tuan, H.-Y. Alkanethiol-Passivated Ge Nanowires as High-Performance Anode Materials for Lithium-Ion Batteries: The Role of Chemical Surface Functionalization. *ACS Nano* **2012**, *6*, 9932–9942.

(41) Hwang, J.; Jo, C.; Kim, M. G.; Chun, J.; Lim, E.; Kim, S.; Jeong, S.; Kim, Y.; Lee, J. Mesoporous Ge/GeO2/Carbon Lithium-Ion Battery Anodes with High Capacity and High Reversibility. *ACS Nano* **2015**, *9*, 5299–5309.

(42) Chockla, A. M.; Klavetter, K. C.; Mullins, C. B.; Korgel, B. A. Solution-Grown Germanium Nanowire Anodes for Lithium-Ion Batteries. *ACS Appl. Mater. Interfaces* **2012**, *4*, 4658–4664.

Figures and Tables

Table 1. Yield and In content of Ge nanowires under different growth conditions.

Precursor type	Synthesis Temp. (°C)	Solvent	Capping ligand	Solvent: OA vol. ratio	TOPO (mmol)	Ge:In molar ratio	Yield	Indium content (at.%)
1	180	*n*-dodecane	TOPO	-	0.5	100:1	81%	1.3 ± 0.1
1	180	*n*-dodecane	OA	1:1	-	100:1	23%	-
1	300	*n*-hexadecane	TOPO	-	0.5	100:1	81%	-
1	300	*n*-hexadecane	OA	1:1	-	100:1	77%	1.6 ± 0.5
1	350	Squalene	OA	1:1	-	100:1	85%	1.8 ± 0.8
1	380	Squalene	TOPO	-	0.5	100:1	-	-
2	350	Squalene	OA	1:1	-	100:1	79%	0.9 ± 0.1

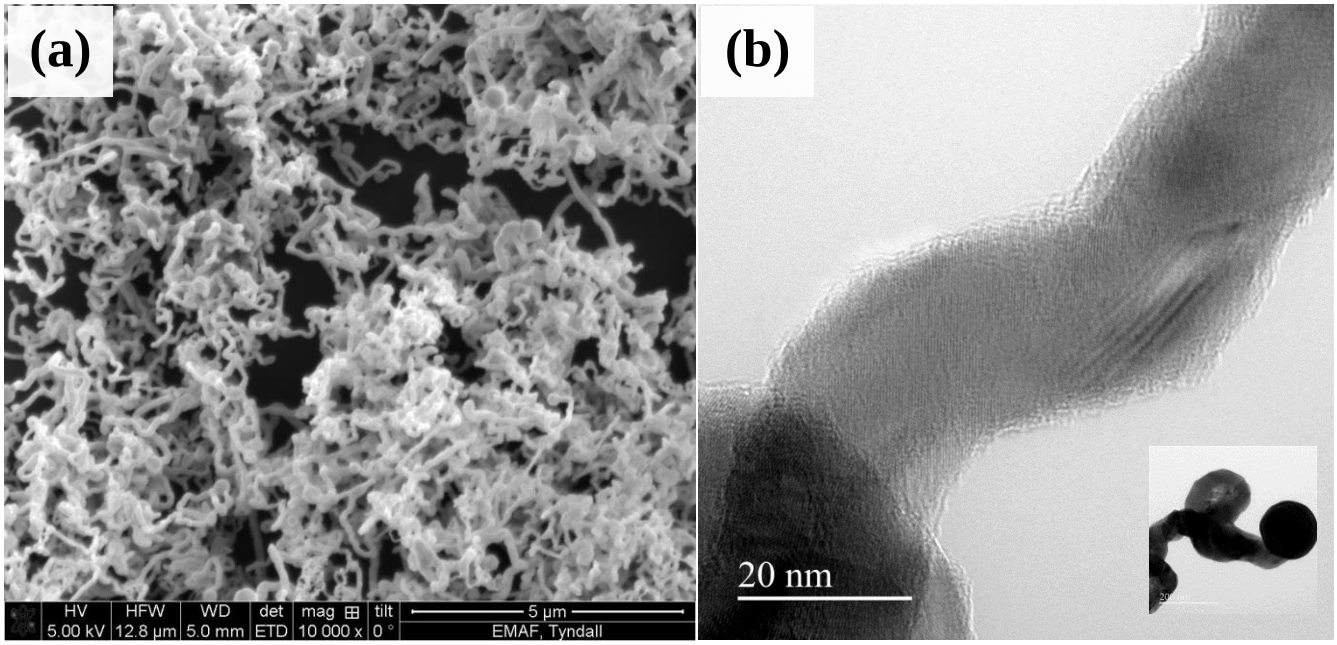

Figure 1. (a) SEM image and (b) high resolution bright field TEM image of Ge nanowires synthesized with precursor **1** in *n*-dodecane, in the presence of TOPO at 180 °C. Inset: In nanoparticle at the tip of a Ge nanowire (scale bar: 200 nm).

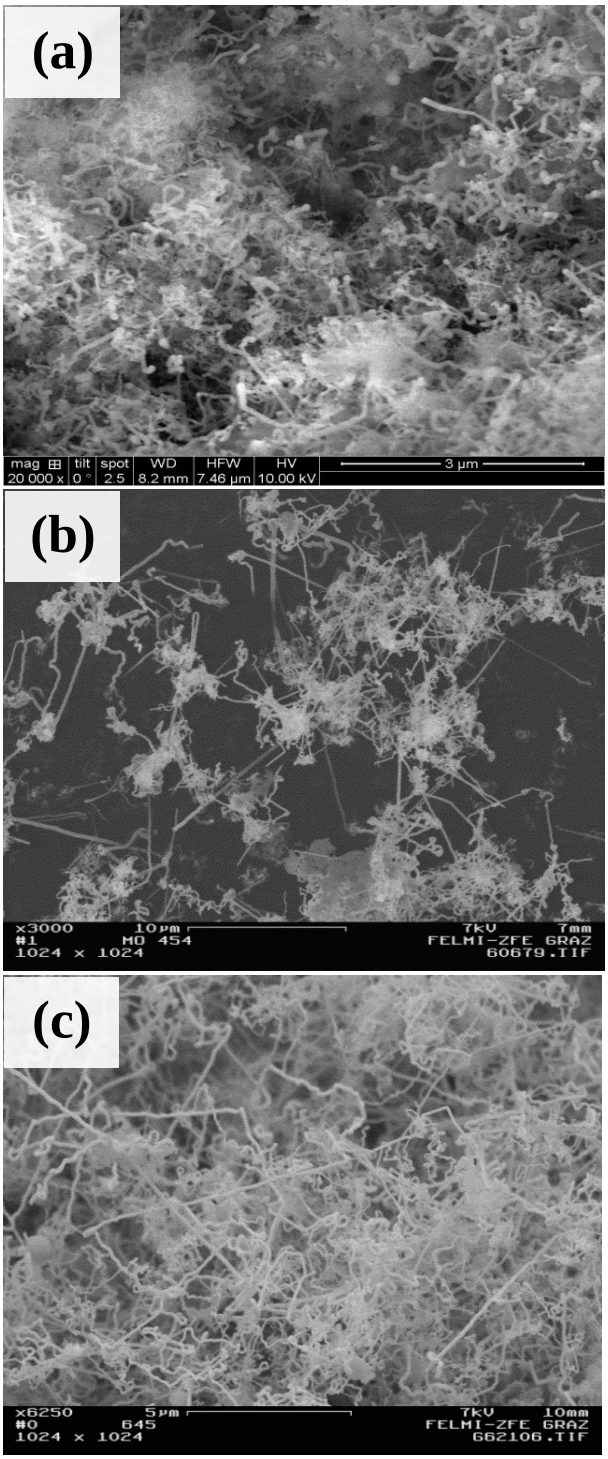

Figure 2. SEM images of Ge nanowires synthesized with precursor **1** in presence of OA. (a) Grown in *n*-dodecane at 180 °C. (b) Grown in *n*-hexadecane at 300 °C. (c) Grown in squalane at 350 °C.

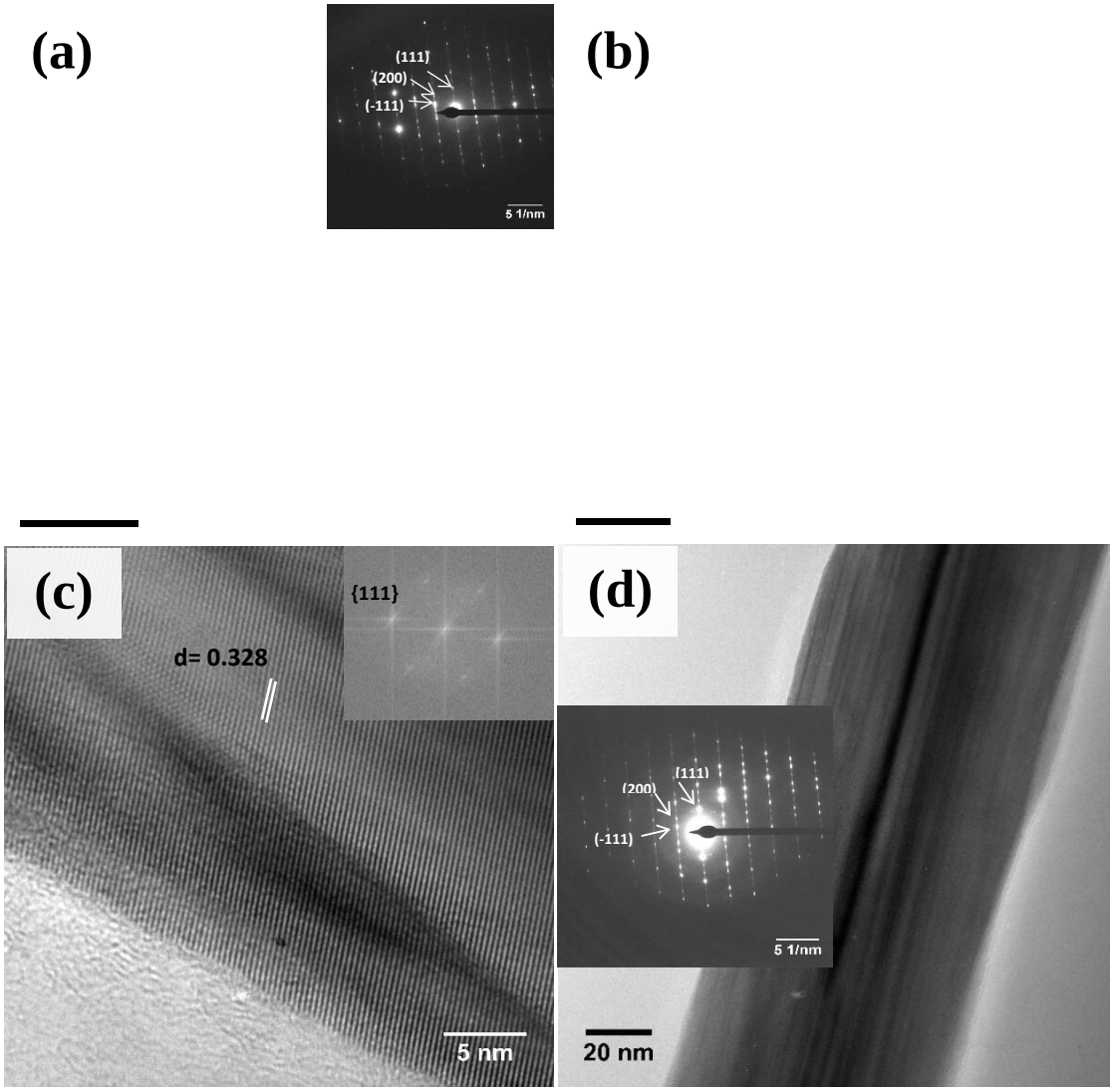

Figure 3. (a) and (b) Bright field TEM images (inset: SAED pattern) of different Ge nanowires prepared with precursor **1** in *n*-hexadecane in the presence of OA at 300 °C, displaying longitudinal stacking faults. (c) and (d) Bright field TEM images of single crystalline (inset: FFT pattern) and defected Ge nanowires (inset: SAED pattern) respectively, prepared with precursor **1** in squalane in the presence of OA at 350 °C. (d) Longitudinal staking faults parallel to the nanowire growth axis.

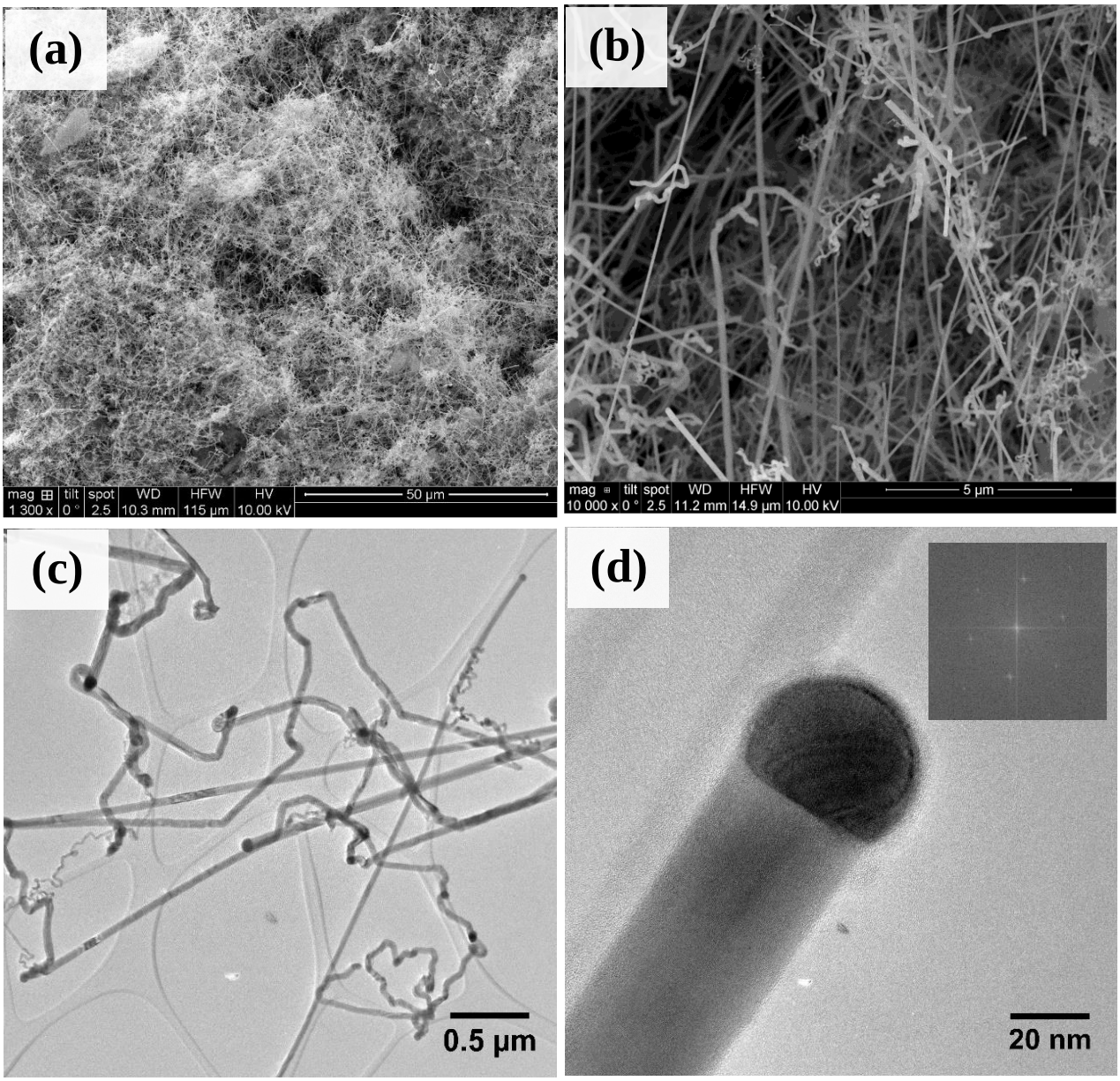

Figure 4. (a) and (b) SEM images of Ge nanowires synthesized with precursor **2** in a squalane:OA mixture at 350 °C. (c) and (d) Bright field TEM images of the same Ge nanowires. (c) Straight and kinked nanowires are shown in the image. (d) In nanoparticle at the tip of a Ge nanowire. FFT pattern in the inset confirms the crystallinity of the nanowire.

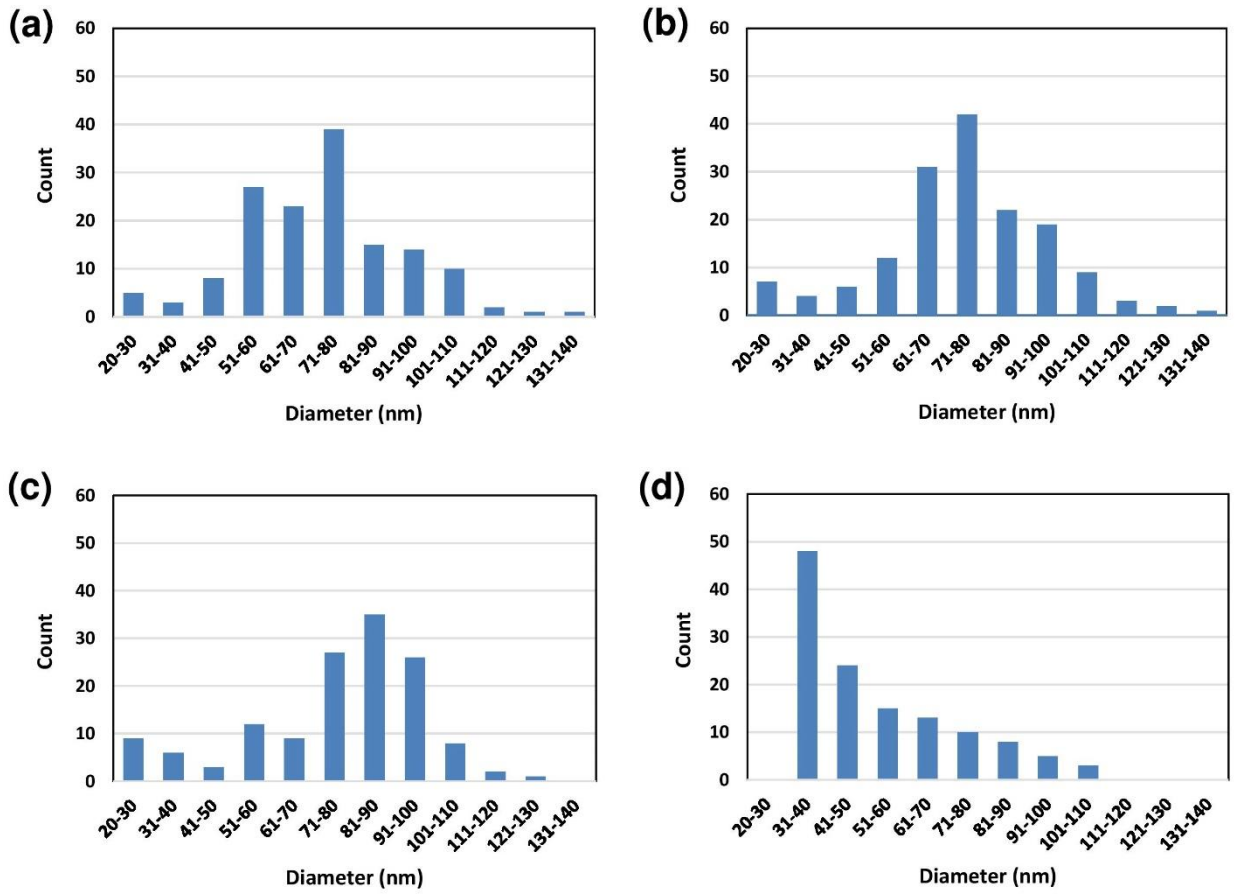

Figure 5. Histograms of the diameter of the Ge nanowires obtained with: (a) Precursor **1** in the presence of TOPO at 180 °C. (b) Precursor **1** in the presence of OA at 300 °C. (c) Precursor **1** in the presence of OA at 350 °C. (d) Precursor **2** in the presence of OA at 350 °C.

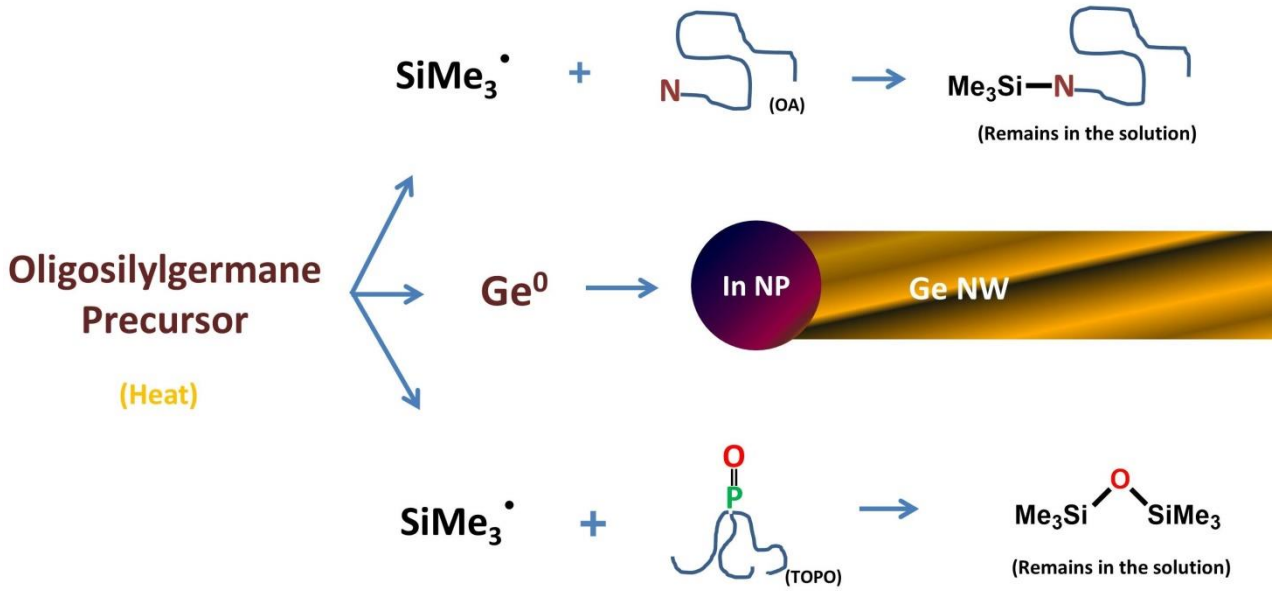

Figure 6. Proposed mechanism involving the thermal decomposition of a oligosilylgermane precursor, the subsequent reaction of TMS groups from the precursor with capping ligands and finally the formation of an In-catalyzed Ge nanowire.

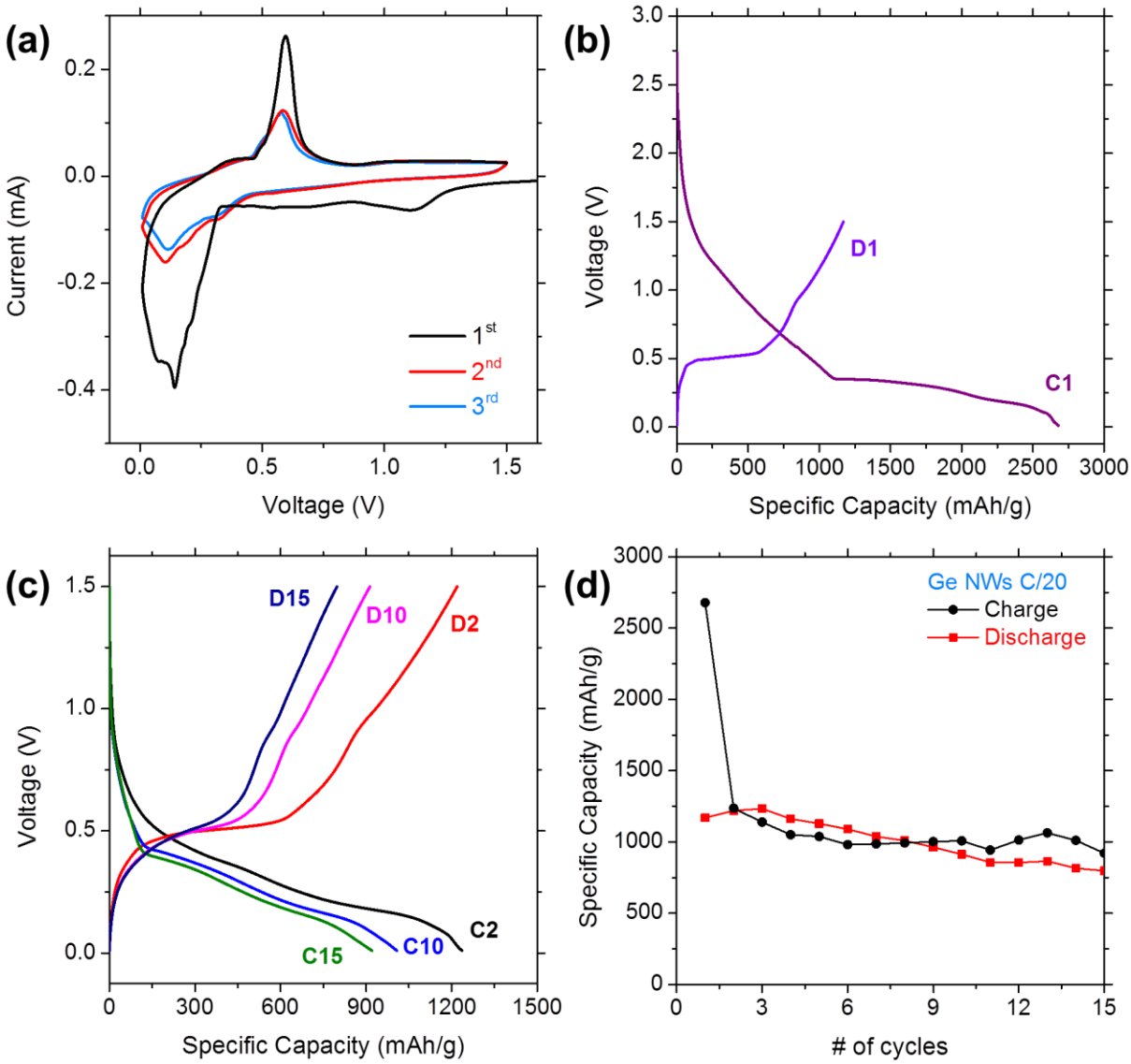

Figure 7. (a) Cyclic voltammograms for Ge nanowires acquired at a scan rate of 0.2 mV s^{-1}. Charge and discharge voltage profiles for (b) the 1st cycle and (c) the 2nd, 10th and 15th cycles for Ge nanowires at a C rate of C/20 in a potential window of 1.5 – 0.01 V. (d) Comparison of the charge and discharge specific capacity values obtained for over 15 cycles.

Table of Contents Figure